Pion-Proton Scattering at 150 and 170 Mev*

J. Ashkin, J. P. Blaser, F. Feiner,† and M. O. Stern
Carnegie Institute of Technology, Pittsburgh, Pennsylvania
(Received August 5, 1955)

The pion-proton differential scattering cross sections have been measured at 150 and 170 Mev. Measurements were made at eight angles using scintillation counters and a liquid hydrogen target. Statistical errors are of the order 5 percent or less. Phase shift analyses of the data have been made on the assumption that the total isotopic spin is conserved and that only s and p waves are appreciably scattered. The angular distributions give no positive indication of any d-wave scattering.

I. INTRODUCTION

THE main features of the pion-proton scattering were established with remarkable clarity by the pioneering experiments of Fermi[1–3] and co-workers at Chicago. Following this work, a number of experiments[4–6] were undertaken to increase the accuracy of the observations and to test Fermi's general conclusions. The energy region near 200 Mev is especially attractive for this purpose since the total cross-section measurements[7,8] with both positive and negative pions have shown that the scattering is large in this range and that the dominance of the isotopic spin 3/2 states, first evident in the lower energy scattering, is still maintained.

In the present experiments at 150 Mev and 170 Mev, we have measured the differential elastic scattering of positive and negative pions and the charge exchange scattering of negative pions for eight angles. This has been done with sufficient accuracy, keeping statistical errors below 5 percent and making all corrections of magnitude 0.5 percent or more, so that the data provide a good test of the charge independence hypothesis and of the supposition that only s and p waves play a significant role in the scattering.

II. MESON BEAMS

The meson beams used for this experiment are produced by the circulating 440-Mev protons inside the cyclotron chamber hitting targets of Be (for π^-) or Cu (for π^+).[7] After emerging from the shield wall the beams are bent through 45° by an analyzing and focusing magnet. Before each run a range curve is taken and analyzed to determine mean energy and beam contaminations. The latter is mainly due to muons, approximately 5 percent in the π^+ beams and 8 percent in the π^- beams. π^- beams are also slightly contaminated by electrons. The exact amount of electrons present proved very difficult to determine, but scattering experiments and range curves made with elements of different atomic numbers showed the contamination to be negligible. Beams of positive mesons are accompanied by protons of the same momentum. Time of flight discrimination is used in this case.[7] The energy spread of the beams is determined from the range curve, taking into account energy straggling due to multiple scattering in the absorber. The total energy spread, including energy loss in the target, is ±7 Mev at both energies. The beam intensities over an area of 25 cm² ranged from 10 000 sec^{-1} for 150 Mev π^- to 80 sec^{-1} for 170 Mev π^+. In order to prevent overloading of the electronic circuits however, measurements were taken at intensities lower than 3000 sec^{-1}.

III. SCATTERING GEOMETRY

The experimental arrangement for scattering (see Fig. 1) is similar to the one used previously by other laboratories.[4,9] The incoming meson beam is defined by a telescope consisting of three counters with total spacing of 150 cm. The first monitor counter, 1, is placed at the exit of the analyzing magnet, the third

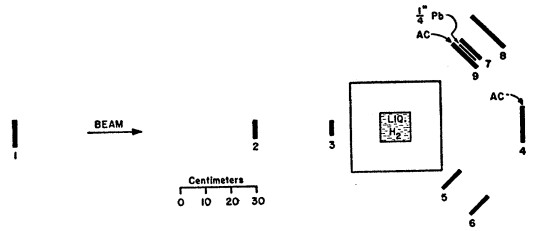

FIG. 1. Experimental arrangement. For the π^- measurements, counters 5 and 6 detect the elastically scattered pions and the telescope of counters 9,7 and 8 (with 9 in anticoincidence) detects the γ rays from the charge exchange scattering. For the π^+ scattering, two detecting telescopes analogous to 5,6 are used to measure the scattered particles on both sides.

* Research partially supported by the U. S. Atomic Energy Commission.

† A thesis based on this work has been submitted by F. Feiner in partial fulfillment of the requirements for the degree of Doctor of Philosophy at Carnegie Institute of Technology.

[1] Anderson, Fermi, Long, Martin, and Nagle, Phys. Rev. **85**, 934 (1952).

[2] Anderson, Fermi, Long, and Nagle, Phys. Rev. **85**, 936 (1952).

[3] Anderson, Fermi, Martin, and Nagle, Phys. Rev. **91**, 155 (1953).

[4] M. Glicksman, Phys. Rev. **94**, 1335 (1954).

[5] H. L. Anderson and M. Glicksman, Phys. Rev. **100**, 268 (1955).

[6] Anderson, Davidon, Glicksman, and Kruse, Phys. Rev. **100**, 279 (1955).

[7] Ashkin, Blaser, Feiner, Gorman, and Stern, Phys. Rev. **96**, 1104 (1954).

[8] S. J. Lindenbaum and L. C. L. Yuan, *Proceedings of the Fifth Annual Rochester Conference on High Energy Physics* (University of Rochester Press, Rochester, 1955) and Phys. Rev. **100**, 306 (1955).

[9] Bodansky, Sachs, and Steinberger, Phys. Rev. **93**, 1367 (1954).

counter, 3, 7 cm wide and 3.5 cm high, defines the beam geometrically. The mesons then traverse a liquid hydrogen target 12 cm deep in the beam direction. This target is built of styrofoam[10] and equipped with a nitrogen jacket reducing evaporation to 300 cm^3 per hour. The chief advantage of the styrofoam construction is the very low probability for conversion of γ rays in the target walls. The hydrogen target is located in the center of the scattering table. Two legs carrying counters revolve around it.

To detect elastically scattered mesons two counters are used, the second one 4 in.$\times$6 in. high, defining the solid angle of 0.08 steradian. At the small angles (30° and 40° in the laboratory system) enough absorber is inserted between the counters to avoid counting the recoil protons produced by backward scattered mesons.

For the detection of the gamma rays produced in charge exchange scattering, the counter arrangement is the following. The gamma rays first traverse an anticoincidence counter, 9, whose purpose is to avoid detection of charged particles. Immediately behind is a $4\frac{1}{2}$ in.$\times 4\frac{1}{2}$ in. lead converter (normally $\frac{1}{4}$ in. thick) defining the solid angle of 0.07 sterad. Conversion electrons are counted by two counters (7 and 8) following the converter. The geometry allows conversion electrons to be counted if emitted into a cone of approximately 40° half-angle.

An anticoincidence counter, number 4, 6 in. in diameter, is placed in the incident beam behind the hydrogen target.[11] Its purpose is to block the detection equipment each time an incident meson is not scattered by the hydrogen and therefore hits the anticoincidence counter. This reduces the chance of random background events in the ratio $t/(1-t)$, t being the fraction of beam transmitted through the hydrogen. (t is approximately 90 percent for π^+, 95 percent for π^-.) Since the transmission into anticoincidence counter 4 is different for full and empty target, a correction factor has to be applied to the empty target counts before one subtracts them from the hydrogen counts. This factor can be obtained by a short measurement of scattering by the dummy target with the anticoincidence disabled. A very considerable improvement in the subtraction was obtained by this method for the negative pion scattering.[12] For π^+ scattering, the advantage was not so great and this counter was not used.

IV. COUNTERS, ELECTRONICS

The counters use plastic scintillators (normally 1 cm thick) produced by the method given by Wouters.[13] As photomultipliers R.C.A. types 5819 and 6199 were used. All counters were shown to be 100 percent efficient to minimum ionizing particles over their entire area. The block diagram of the electronics used is shown in Fig. 2. The fast multiple-coincidence circuit uses G-7A germanium diodes in DeBenedetti-type[14] circuits. The use of the semifast secondary coincidence circuit[7] makes it possible to keep detection efficiencies extremely constant over long periods of time and helps define corrections due to deadtime.

V. EXPERIMENTAL PROCEDURE

The rather short distance from the target to the defining counter detecting the scattered mesons requires a careful centering of the incoming beam. Profiles of the beam were taken with a small ($\frac{1}{2}$ in. diameter) sampling counter. In addition, measurements were taken for scattering both left and right during the same run. For positive pions elastic scattering was measured on both sides simultaneously with identical geometry. In the case of negative mesons, simultaneous measurements of elastic and charge-exchange scattering were performed, then the detecting legs reversed to the opposite sides and the same points retaken. The average between cross sections obtained on the left and right is considered free of effects due to possibly poor beam centering. Measurements were usually made at eight angles, the points for full and empty target being alternated sufficiently to avoid errors due to drifts and especially changes in cyclotron operation.

Total cross sections were also determined during the experiment for each of the energies using the transmission method.[7] The final detecting counter used was 8 in. in diameter and placed 60 cm from the center of the hydrogen, thereby subtending a half-angle of 9.8°.

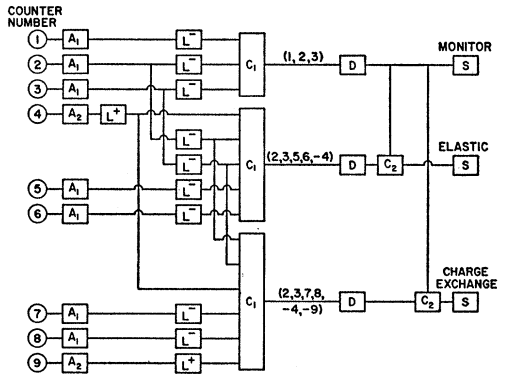

FIG. 2. Block diagram of the electronics. A_1—100-Mc bandwidth amplifier; A_2—40-Mc band width amplifier; L^- limiter and clipper; L^+ limiter; C_1 fast diode coincidence circuit of approximately 5-mμsec resolving time; D fast discriminator and univibrator pulse shaper; C_2 semi-fast coincidence circuit of approximately 20-mμsec resolving time; S fast 0.1-μsec scaler.

[10] F. Feiner and J. A. Kane, Carnegie Institute of Technology Report (unpublished).

[11] A. Roberts and J. Tinlot, Phys. Rev. **90**, 951 (1953).

[12] When observing scattering of π^- at large angles (157.5° in the laboratory system), recoil protons may produce counts in anticoincidence counter 4. Sufficient absorber is therefore placed in front of the anticoincidence counter to stop the protons. This increases the detection efficiency for neutrons but the net correction is still negligible because of the small solid angle.

[13] L. Wouters (private communication).

[14] S. DeBenedetti and H. Richings, Rev. Sci. Instr. **23**, 27 (1952).

VI. EFFICIENCY OF γ-RAY DETECTION

The problem of assigning an absolute efficiency to the conversion telescope which detects the γ rays from π^0 decay is rather complicated because of the wide energy spectrum of the γ rays and the complex multiple processes suffered by the electrons and positrons after creation in the lead converter. Ideally, the telescope should have been calibrated with an extended source of monochromatic γ rays whose energy could be varied from 20 to 300 Mev, the energy range of the π^0 γ rays in the laboratory. Since this was not possible we decided to use the Monte Carlo calculations of Wilson[15] on photon initiated showers as a basis for the energy dependence of the efficiency, and to rely on several independent empirical determinations for the absolute value.

Figure 7 of Wilson's paper gives the expected number n of electrons with energy greater than 8 Mev in the core of a shower and within 30° of the incident photon direction, plotted against penetration in lead for initial photon energy in the range 20–500 Mev. The probability for finding no electrons is shown to be well represented by $\exp(-n)$. Since our telescope is sensitive to one electron and since the geometry is comparable to Wilson's, the detection efficiency would be $1-\exp(-n)$. Although the energy dependence of this expression is probably accurate enough for our purpose, the absolute value is expected to be too high for all except the central portion of the lead converter, since showers initiated near the edges of the lead give rise to some fraction of electrons missing the final counter. To estimate the magnitude of this effect we made some experiments with the Panofsky γ radiation (see below), using a centrally located lead converter of small cross-sectional area, varying the distance between converter and final counter to obtain a rough angular distribution of the electrons.[16] With this distribution we could attribute an effective detection efficiency to each point of the actual lead converter, which, upon averaging gave 0.81 as the overall reduction factor to be applied to $1-\exp(-n)$.

A second estimate of this reduction factor was based on a measurement of the absolute efficiency for detecting the spectrum of the Panofsky γ rays[17] emitted when negative pions at rest are captured by protons. Figure 3 shows the experimental arrangement used. Transmissions with and without hydrogen in the Dewar were recorded simultaneously with counts in the γ-ray telescope as a function of the copper thickness used to bring the mesons to rest. From the differentiated range curves or from the difference between the hydrogen-out–hydrogen-in transmissions, we can obtain the number

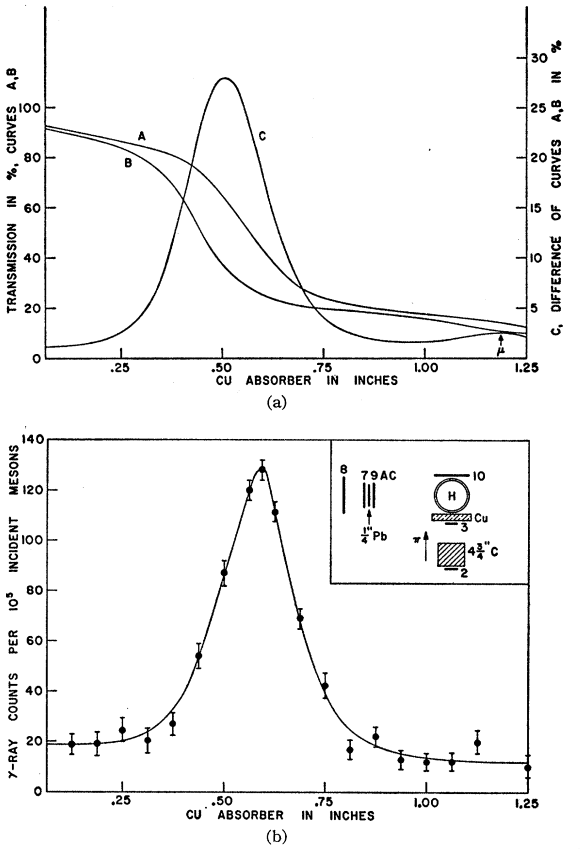

FIG. 3. Detection of the Panofsky γ rays. The experimental arrangement is shown in the inset next to the lower curve which gives the γ-ray counts for different thicknesses of Cu absorber. Curve A in the upper part of the figure gives the transmission curve for empty Dewar, curve B the same with Dewar containing hydrogen. Curve C is the difference between A and B and should be compared in shape with the γ-ray curve below it.

of pions stopping in the hydrogen and hence the number of γ rays emitted into the solid angle subtended by the lead converter. Comparison with the observed counts in the telescope gives the efficiency. The different methods for analyzing the range curves agree well with one another to give an efficiency of 42 ± 3 percent, or equivalently a reduction factor 0.79 ± 0.05. An indication of the reliability of the procedure is provided by the fact that the peak in the γ-intensity curve has very nearly the same shape as the peaks in the differentiated range curves or in the transmission difference curve shown in Fig. 3. It should be remarked that in order to obtain this similarity in peak shape and to get reproducible values for the number of pions stopping, it was necessary to make the absorption geometry as compact as possible to reduce the effect of multiple scattering of pions near the end of their range.[18]

A third determination of the absolute value of the

[15] R. R. Wilson, Phys. Rev. **86**, 261 (1952).

[16] The rather sharp decrease in the number of electrons beyond 30 or 35 degrees gave an indication of the applicability of Wilson's results.

[17] Panofsky, Aamodt, and Hadley, Phys. Rev. **81**, 565 (1951). A similar calibration was made in the first experiments of Anderson, Fermi *et al.* (reference 3).

[18] A glass Dewar was used to decrease the distance from the copper absorber to the last counter. The additional absorber represented by the exit walls of the Dewar and part of the last counter produces a relative shift of the peaks in Fig. 3.

efficiency can be made by comparing the measured total cross section for π^- scattering with the sum of the integrated elastic and charge exchange differential cross sections. From this comparison at 150 Mev and 170 Mev, we found 0.81 ± 0.04 as the reduction factor.

Table I gives the absolute efficiency[19] and the estimated error finally adopted for the detection of the γ rays at each laboratory angle for the two incident pion energies. The efficiency is defined here as the ratio of counts in the conversion telescope to number of γ rays striking the lead converter. Actually, it is not possible to give an *a priori* efficiency for each angle since the energy spectrum of the π^0 decay γ rays depends on the angular distribution of the π^0 scattering which it is desired to measure. We have nevertheless found it convenient to calculate an average efficiency at each angle for a γ-ray spectrum based on an *assumed* π^0 angular distribution, close to the actual one. Using these efficiencies one can go from the measured γ counts at each angle to a *calculated* π^0 angular distribution,[3] and upon repetition of the process obtain a second approximation to the average efficiency, and so on. In practice, the iteration procedure converged very rapidly.

VII. CORRECTIONS AND ERRORS

Since the experiment was done with counting statistics of the order of 3–5 percent, there are a number of corrections that have to be made. Corrections of less than 0.5 percent are considered negligible.

We can divide the corrections into those that are (rigorously or practically) angle-independent, and those that are angle-dependent. Uncertainties in the former do not affect the shape of the angular distribution and should therefore be included in a bracket pertaining to the normalization of the cross sections. Uncertainties in the angle-dependent corrections must be compounded at each angle with the statistical counting errors.

We can further subdivide corrections according to whether they are common to all three scattering processes, or pertinent to only one or two of them. Energy dependence of the corrections is, of course, taken into account whenever significant.[20] Table II shows the magnitude of the corrections for elastic π^- scattering at 150 Mev. The corrections are identified by numbers referring to the list below. They are given in the form of factors by which the raw data must be multiplied, even though some are inherently additive and can be expressed as factors only in terms of specific measurements. Uncertainties in corrections are quoted whenever significant. The Coulomb effect will be discussed separately in Sec. VIII.

TABLE I. Efficiencies for γ-ray detection.

Lab. angle (degrees)	Efficiency 150 Mev		Efficiency 170 Mev	
30°	0.475 ±0.03	1.02	0.485 ±0.03	1.02
40°		1.00		1.00
55°		0.96		0.96
76°		0.92		0.92
98°		0.91		0.91
123°		0.92		0.92
141°		0.94		0.94
157.5°		0.96		0.96

[19] A small correction for conversion of γ rays in the target and in the anticoincidence counter is included in these values.

[20] For detailed derivations of the corrections, see F. Feiner, thesis, Carnegie Institute of Technology, May, 1955 (unpublished).

A. Angle-Independent Corrections

The following corrections 1 to 4 are common to all three processes; 5 concerns elastic scattering and 6 concerns charge-exchange scattering.

1. The pion beams are contaminated by muons. Some of these are selected by the deflecting magnet to have the same momentum as the pions, and form a shoulder on the integral range curves. A small number come from pions decaying in flight after the magnet. The percent contamination is obtained from the shoulder of the range curves under the assumption that muons suffer no nuclear interactions. It ranges from 5 to 8 percent. Because of uncertainties in this determination, as well as in contamination by electrons and protons, a standard deviation of 2 percent is assigned to the cross sections.

2. The incident beam is attenuated in the hydrogen target, so that the beam effective for scattering is somewhat lower than the monitored beam. What is relevant is obviously the beam intensity at the center of the hydrogen target.

3. The incident beam may be scattered out or absorbed by the third monitor counter and the target wall. This makes the measured cross section too low. Accidental coincidences in the monitor act in the same direction; dead time losses in the slow coincidence circuit have the opposite tendency. The net result is that the cross sections should be raised by an estimated (1.5 ± 1.0) percent.

4. The dimensions of the hydrogen container are known to within 1.5 percent.

5. Elastically scattered pions of both signs can be scattered or absorbed in the first detecting counter or the target wall. In addition the efficiency of the detecting telescope may be somewhat below 1.00. Because of these effects the elastic cross sections should be raised by (2 ± 1) percent.

6. In charge exchange scattering one of the γ rays resulting from π^0 decay is occasionally internally converted[21] and therefore not detected, causing the measured cross section to be 0.7 percent low.

B. Angle-Dependent Corrections

The following corrections 7 through 10 concern all three processes; 11, 12 and 13 pertain to elastic scattering, 14 through 17 to charge-exchange scattering.

[21] Lindenfeld, Sachs, and Steinberger, Phys. Rev. 89, 531 (1953).

TABLE II. Typical set of correction factors for elastic scattering of 150-Mev π^-. θ is the laboratory angle; numbers refer to the list of Sec. VII.[a]

θ	7.	8.	9.	10.	11.	12.	Total
30°	1.010	0.995	1.011±0.010	0.983	1.047±0.010	0.959±0.007	1.003±0.016
40°	1.012	1.000	1.010±0.010	0.988	1.021±0.010	0.958±0.007	0.988±0.016
55°	1.017	0.995	1.008±0.010	0.990	...	0.936±0.009	0.945±0.013
76°	1.021	0.980	1.005±0.010	0.985	...	0.895±0.018	0.886±0.021
98°	1.021	1.003	1.003±0.010	0.979	...	0.877±0.021	0.882±0.023
123°	1.017	1.004	1.001±0.010	0.978	...	0.885±0.019	0.885±0.021
141°	1.012	1.004	0.999±0.010	0.983	...	0.910±0.015	0.908±0.018
157.5°	1.008	1.000	0.999±0.010	0.901	...	0.914±0.014	0.829±0.017

[a] Angle-independent corrections are 1: 1.080±0.020, 2: 1.013, 3: 1.015±0.010, 4: 1.000±0.015, and 5: 1.020±0.010. Total: 1.133±0.029.

7. The solid angle subtended by the defining detecting counter or Pb converter at the target is crudely equal to the counter or converter area divided by the distance squared from target center to detector center. A correction arises from the fact that the detector is a plane rectangle and that the irradiated part of the target has a rectangular cross section in the scattering plane.

8. The angular resolution used in the experiment (±7°) is large enough to give a sizable correction to the angular distribution where it is strongly curved.

9. Double elastic scattering of mesons may occur within the hydrogen. Since the scattering is far from isotropic and strongly energy-dependent, this gives rise to an angle-dependent correction. In the forward direction the measured distributions are depleted by this effect; backward they are augmented. In the π^+ case, these effects amount to 2 percent for the forward and backward angles. In the π^- case, there is, furthermore, the possibility of an elastic-charge exchange type of double scattering which enhances the measured charge exchange distribution and reduces that for elastic scattering. An uncertainty of ±1 percent in cross sections is assigned to these corrections.

10. The presence of hydrogen in a full target modifies the scattering from the target walls, so that one cannot simply subtract the dummy counts from the hydrogen counts to obtain the hydrogen effect. Instead, the dummy counts must be multiplied by a factor different from unity before being subtracted. We distinguish three effects:

(a) When the target is full, attenuation of mesons in the hydrogen causes fewer mesons to reach the far target wall and to scatter from it than would do so were the target empty. For π^+ scattering, this effect requires an upward correction in the cross section of order 1 percent. For π^- scattering, it is negligible.

(b) In π^- scattering, fewer mesons reach anticoincidence 4 (see Fig. 1) when the target is full, so that the accidental rate is increased. The dummy counts must therefore be multiplied by a factor greater than unity (see Sec. III) which is found not to exceed 1.05 for elastic, 1.20 for charge exchange scattering.

(c) Mesons scattered doubly, once in the hydrogen, and once in the target walls, give a negligible correction.

11. The absorption of mesons in the lucite proton absorbers used at small angles was measured by putting the detecting telescope in the beam. An uncertainty of ±1 percent in the cross section is assigned to this correction.

12. The detecting telescope for elastically scattered π^- mesons is somewhat sensitive to γ rays converted in the target, its walls, or the first detecting counter. To correct for this, one has to estimate the relative γ-ray sensitivity of the elastic and charge exchange detectors. The correction at a given angle amounts to about 6 percent of the charge exchange counts at the same angle, and is considered uncertain to one part in six.

13. $\pi-\mu$ decay following a scattering event may alter the angular distribution. The correction can be shown to be negligible since only a few percent of the pions decay and their muons are emitted in a narrow forward cone about the pion direction.

14. The efficiency ϵ for γ-ray detection is discussed in Sec. VI and includes such corrections as the conversion of γ rays in the target or anticoincidence counter. ϵ is thought to be known to ±0.03.

15. The radiative capture reaction $\pi^-+p\rightarrow\gamma+n$ should be excluded. Using CalTech data on the photopion production on protons[22,23] and on deuterons, one finds a correction of order 1–2 percent.

16. The neutron from the charge-exchange reaction has a chance of being counted in the charge exchange detector, by changing to a proton in the converter or first coincidence counter. The correction amounts to 3 percent at 30° and rapidly goes to zero at larger angles. The presence of Lucite stoppers prevents the detection of these low-energy neutrons in the elastic scattering detector.

17. The chance for detection, in anticoincidence 4, of a neutron or γ ray correlated with a γ ray that would otherwise have registered a count in the detector is negligible.

[22] R. L. Walker, *Proceedings of the Fourth Annual Rochester Conference on High Energy Physics* (University of Rochester Press, Rochester, 1954) and R. F. Bacher *et al.*, Phys. Rev. **92**, 1090(A) (1953).

[23] Sands, Teasdale, and Walker, Phys. Rev. **95**, 592 (1954).

VIII. PROCESSING OF DATA

Our aim is to apply every relevant correction to our data and present them in such a form that they can be fed to a machine for computation of phase shifts. At the same time we shall wish to make an approximate phase-shift analysis[24] ourselves, and so need to express the differential center of mass cross sections in the form

$$\sigma(\theta)=[1.00\pm\delta]\times\{(a\pm\delta a)+(b\pm\delta b)\cos\theta+(c\pm\delta c)\cos^2\theta\}, \quad (1)$$

where the normalization bracket [ ] collects all uncertainties not affecting the angular distribution.

In Sec. VIII, A, we shall discuss how the data are averaged and normalized. In Sec. VIII, B, we shall briefly show why and how a Coulomb correction is applied. Evidence justifying our neglect of d waves will be presented in Sec. VIII, C.

A. Averaging of Data

The data of a given π^+ run are processed to yield the net hydrogen effect at each angle, and multiplied by the appropriate factor to convert them to cross sections in the center of mass system. A weighted average of all runs[25] is made, all corrections are applied, and the statistical errors of the cross sections are compounded with the uncertainties in the angle-dependent corrections.

A least squares fit to the form (1) is then made, so that a, b, c and their errors δa, δb, δc are determined. Integration yields a total cross section $4\pi(a+c/3)$. A second, independent measurement of the total cross section by transmission is available (see Sec. V). A comparison of these cross sections is given in Table III. Since the two values are in good agreement, our procedure is to normalize the differential cross sections in such a way that their integral equals the weighted average[26] of the two total cross-section values. Table IV gives the final differential cross sections (without and with the Coulomb correction described in Sec. VIII, B). Table VI gives the final coefficients a, b, c (including the Coulomb correction). The procedure is the same for the π^- data, except for the following points:

1. For charge exchange scattering the coefficients a,b,c derived from the γ-ray distribution in the center-of-mass system are used to deduce the coefficients for the π^0 distribution following the iteration procedure outlined in Sec. VI.[27]

2. For both elastic and charge exchange scattering, the normalization factors are now dependent on the γ-detection efficiency in addition to the total cross section, so that the systematic deviations δ of (1) are somewhat larger than for π^- scattering.

The final differential cross sections are contained in Tables IV and V and the coefficients a,b,c are given in Table VI.

TABLE III. Total cross sections.

Energy (Mev)		Total cross section (mb) From integration	From transmission	Coulomb correction (mb)
150	π^+	166.6±5.0[a] (2.5)[b]	164.5±4.6[a] (1.8)[b]	1.1[c]
	π^-	...[d]	55.3±1.6[a] (0.5)[b]	−1.4[c]
170	π^+	201.6±6.0[a] (2.9)[b]	194.9±5.5[a] (2.2)[b]	0.5[c]
	π^-	...[d]	62.7±1.9[a] (0.6)[d]	−1.1[c]

[a] Final estimated error obtained by combining uncertainty in beam contamination and hydrogen thickness with error quoted in b.
[b] Statistical error for transmission or compound of statistical errors with uncertainties in angle dependent corrections for cross section obtained by angular integration.
[c] To be added to the uncorrected transmission cross section in order to eliminate the Coulomb interference for scattering outside the acceptance cone of the last counter. This correction is included in the final values quoted in the table. (see Sec. VIII). The Coulomb correction has also been applied to the total cross section obtained by integration.
[d] The efficiency of the γ-ray telescope has been partly determined by requiring agreement between the cross sections obtained by transmission and by integration of the elastic and charge exchange angular distributions.

B. Coulomb Effect

Although the interference between the Coulomb and nuclear scattering of the pion is of importance mainly at small angles, the magnitude of the effect is quite comparable to the quoted errors in the differential cross section up to 50 degrees or more in the center-of-mass system. This is especially true for the π^- elastic scattering where the nuclear scattering amplitude is relatively small. To extract the purely nuclear scattering from the observed differential cross sections it is sufficiently accurate to make a correction based on scattering phase shifts deduced[24] from the uncorrected data. The signs of these phase shifts are chosen to agree with the small-angle Coulomb interference experiments of Orear[28] and Puppi.[29]

Let us, for simplicity, illustrate the Coulomb problem[30–32] by considering π^+ scattering. The purely nuclear scattering cross section in s and p states can

[24] J. Ashkin and S. Vosko, Phys. Rev. **91**, 1248 (1953).
[25] This excludes certain runs at the beginning of the experiment during which electronic difficulties prevented our obtaining reliable absolute differential cross sections. These runs were normalized separately before being pooled with the remaining ones.
[26] The weights are obtained, on the one hand, from the statistical error in the transmission measurement, on the other, from the error derived for $(a+c/3)$ in the least squares analysis. The error in the averaged cross section is then combined with the uncertainties in the angle-independent corrections. The resultant relative error is the δ of (1), and constitutes the systematic error that applies to all points of the differential cross section.
[27] Another method, described by Bodansky, Sachs, and Steinberger, Phys. Rev. **93**, 1367 (1954) (based on averaging the γ-ray detection efficiency beforehand for the γ-energy spectrum associated with each Legendre polynominal in the π^0 angular distribution) allows a *direct* determination of the π^0 coefficients a,b,c from the observed γ-ray counts. This method gave the same results as the iteration procedure.
[28] J. Orear, Phys. Rev. **96**, 1417 (1954).
[29] G. Puppi, *Proceedings of the Fifth Annual Rochester Conference on High Energy Physics* (University of Rochester Press, Rochester, 1955).
[30] L. Van Hove, Phys. Rev. **88**, 1358 (1952).
[31] J. Ashkin and L. Smith, Technical Report No. 1, Carnegie Institute of Technology, 1953 (unpublished).
[32] F. T. Solmitz, Phys. Rev. **94**, 1799 (1954).

TABLE IV. Differential cross sections for elastic scattering (in mb/sterad).

	c.m. angle (degrees)	$\pi^+\to\pi^+$	$(\pi^+\to\pi^+)_{\text{nuclear}}$	$\pi^-\to\pi^-$	$(\pi^-\to\pi^-)_{\text{nuclear}}$
a	31.8	19.1±2.8	19.6±2.8	...	...
	37.9	14.5±1.0	14.9±1.0	2.84±0.11	2.57±0.11
	50.1	13.3±0.5	13.4±0.5	2.23±0.07	2.10±0.07
	67.6	8.9±0.4	8.9±0.4	1.35±0.05	1.30±0.06
	90.5	8.0±0.4	8.0±0.4	0.96±0.05	0.95±0.05
	104.6	1.00 ±0.03 8.5±0.6	1.00 ±0.03 8.4±0.6	1.00 ±0.05 ...	1.00 ±0.05 ...
	112.2	11.6±0.7	11.5±0.7	1.13±0.05	1.14±0.05
	134.7	17.4±0.6	17.3±0.6	1.68±0.07	1.70±0.07
	149.6	21.7±0.8	21.6±0.8	1.81±0.09	1.83±0.09
	162.7	25.3±0.8	25.2±0.8	2.06±0.16	2.09±0.16
	169.2	27.4±2.3	27.2±2.3	...	...
b	32.1	19.4±1.6	19.7±1.6	...	...
	38.3	20.2±1.0	20.3±1.0	2.86±0.14	2.65±0.14
	50.7	16.7±0.7	16.8±0.7	2.58±0.09	2.48±0.09
	68.3	11.6±0.6	11.6±0.6	1.57±0.08	1.53±0.08
	91.1	1.00 8.9±0.5	1.00 8.9±0.5	1.00 1.04±0.06	1.00 1.03±0.06
	113.1	±0.03 11.4±0.6	±0.03 11.4±0.6	±0.05 1.31±0.08	±0.05 1.32±0.08
	135.3	21.8±0.8	21.7±0.8	1.87±0.12	1.88±0.12
	150.1	26.7±0.9	26.6±0.9	2.49±0.13	2.51±0.13
	163.0	26.5±1.1	26.5±1.1	3.14±0.24	3.16±0.24
	169.4	28.4±4.8	28.3±4.8	...	...

[a] Measurements at 150±7 Mev. [b] Measurements at 170±7 Mev.

be written[33]

$$\frac{d\sigma(+)}{d\Omega}=\left|\frac{1}{2ik}A+\frac{1}{2ik}B\cos\theta\right|^2+\left|\frac{1}{2ik}C\sin\theta\right|^2,$$

where the first term represents scattering without spin flip. A,B, and C are defined in terms of the isotopic spin 3/2 phase shifts, α_3 for the $s_{1/2}$ state, α_{31} for the $p_{1/2}$ state, and α_{33} for the $p_{3/2}$ state, by

$$A=\Delta(\alpha_3),\quad B=2\Delta(\alpha_{33})+\Delta(\alpha_{31}),\quad C=\Delta(\alpha_{33})-\Delta(\alpha_{31}),$$

where $\Delta(\alpha)$ stands for $\exp(2i\alpha)-1$.

It has been shown[30,31] that at our energies the Coulomb effect is sufficiently taken into account if one adds to the non-spin-flip amplitude for nuclear scattering the Born Coulomb amplitude $\alpha/[2k\sin^2(\theta/2)]$ with the proper (for π^+, negative) sign. Here α is the fine structure constant with c replaced by the velocity of the incoming pion in the laboratory.[32] Note that since the Born amplitude is real, it interferes with $1/(2k)$ $\mathrm{Im}(A+B\cos\theta)$. The interference is most important at small angles, where $A+B\cos\theta\approx A+B$. With the help of relations (6a) and (7) of reference 24, it is easy to see that $\mathrm{Im}(A+B)$ is an experimental constant related to the coefficients a,b, and c of (1), and therefore, independent of the set of phase shifts which may be chosen to represent the data.

To correct for Coulomb effects, the angular distribution for a given process at a given energy is calculated, once including the Coulomb amplitude, and once without it. The difference is the correction that must be applied at each angle in the differential cross section. The difference must also be integrated over all solid angles (excluding that of the detecting counter) and applied as a correction to the transmission measurement of the total cross section (see Table III). The differential cross sections are then again normalized and a last analysis is made from which the final phase shifts can be found. Table IV shows the purely nuclear cross sections and the observed differential cross sections side by side. For the 150-Mev π^- elastic scattering at the smallest angle, the correction is as large as 10 percent.

[33] For notation, see references 24 and 3.

C. d-Wave Evidence

Our treatment of the data is based on the assumption that only s and p waves scatter strongly. If, for example, it were somehow known that d waves make a significant contribution at 150–170 Mev, we should have ten phase shifts to calculate instead of six, and

TABLE V. Charge exchange differential cross sections. (in mb/sterad).

c.m. angle (deg)		$\pi^-\to\gamma$
	150±7 Mev	
36.6		5.09±0.12
48.4		4.52±0.11
65.4		4.28±0.12
87.9		4.53±0.13
109.6	(1.00±0.05)	5.35±0.15
132.4		7.23±0.20
147.9		7.98±0.22
161.6		8.97±0.26
	170±7 Mev	
37.0		6.51±0.16
48.9		5.73±0.15
66.1		5.12±0.15
88.8		5.07±0.14
110.5	(1.00±0.05)	5.62±0.18
133.1		7.82±0.23
148.4		8.46±0.27
162.0		9.47±0.31

TABLE VI. Coefficients a,b,c in least squares fits $d\sigma/d\Omega=a+b\cos\theta+c\cos^2\theta$ (in mb/sterad) and associated M values.[a]

	150±7 Mev			
	$\pi^+\to\pi^+$	$\pi^-\to\pi^-$	$\pi^-\to\gamma$	$\pi^-\to\pi^0$
a:	1.00	1.00	1.00	1.00
b:	±0.03	±0.05	±0.05	±0.05
c:				
	7.66±0.26	0.97±0.03	4.51±0.09	1.54±0.07
	−2.35±0.37	0.44±0.05	−1.79±0.09	−1.34±0.06
	16.47±0.71	1.87±0.10	2.98±0.20	3.63±0.20
	$M=8.1$[a]	$M=14.4$	$M=3.9$	
	$M_0=8$[b]	$M_0=5$	$M_0=5$	
	170±7 Mev			
	$\pi^+\to\pi^+$	$\pi^-\to\pi^-$	$\pi^-\to\gamma$	$\pi^-\to\pi^0$
a:	1.00	1.00	1.00	1.00
b:	±0.03	±0.05	±0.05	±0.05
c:				
	8.88±0.34	1.06±0.04	4.98±0.10	1.69±0.08
	−1.18±0.45	0.42±0.07	−1.16±0.11	−0.84±0.08
	20.46±0.87	2.44±0.13	3.73±0.24	4.25±0.23
	$M=17.3$	$M=9.7$	$M=9.7$	
	$M_0=7$	$M_0=5$	$M_0=5$	

[a] $M=\sum_{i=1}^{n}\epsilon_i^2$ where ϵ_i = deviation of experimental point i from curve, expressed in terms of the error.

[b] Expected value of M is $M_0=n-m$, where n = number of angles at which measurements are made, and m = number of parameters of curve (here three).

would make a five-constant analysis of our data, up to the fourth power in $\cos\theta$. Of the two new terms, the one proportional to $\cos^3\theta$, arising from the interference of d waves and the strongly scattered p waves, might be expected to show up first.

If the three-constant fit (quadratic polynominal in $\cos\theta$), is good, there is little reason to believe that a fourth constant times $\cos^3\theta$ will make the fit significantly better. Clearly the three-constant fit can be made as good as one wishes, if one is willing to increase the angle-dependent uncertainties unduly. This we have taken care to avoid, because the presence of any small amount of d wave would then be completely masked.

One can hope to improve the fit by means of a fourth constant when it is poor. It may be poor for a number of reasons: (1) Higher wave scattering is present; (2) Angle-dependent errors have been underestimated; (3) Statistical fluctuations not previously mentioned cause scatter in the data.[34] To eliminate (3) as a possible cause, we have made a statistical analysis of the π^- data, where, especially at 150 Mev, a large number of runs are available. Application of the χ^2 test[35] to the sums of squares of the deviations of the cross sections from the mean values at each angle showed that the fluctuations were adequately accounted for by counting statistics alone. Thus (3) is ruled out.

TABLE VII. Phase-shifts sets (in degrees).

	150 Mev				170 Mev	
	A_1[a]		A_2[a]		$A_1=A_2$	
α_3	−11.5		−52.5		−12.1	
	F[b]	Y[b]	F	Y	F	Y
α_{33}	52.9	23.0	34.5	20.3	66.2	45.5
α_{31}	−5.9	81.7	12.6	42.0	−11.5	123.3
α_1	8.4		8.8		8.5	
					F	Y
α_{13}	1.5		−0.2		4.6	2.4
α_{11}	1.5		−0.2		1.2	5.8
	↓[c]				↓[c]	
α_3	−10				−8	
α_{33}	51.5				65	
α_{31}	−5				−8	
α_1	9				10	
α_{13}	2				2	
α_{11}	−2				0	

[a] Points A_1 and A_2 refer to the graphical method (reference 24).
[b] F and Y represent Fermi- and Yang-type sets, respectively.
[c] Improved set of phase shifts (see Sec. IX) used for comparison with experimental data in Fig. 4 and Fig. 5.

Table VI gives an indication of the quality of the three constant fits to the experimental data. The quantity $M=\sum\epsilon_i^2$, where the ϵ_i are the deviations of the experimental points from the proposed quadratic expression in $\cos\theta_i$ (in units of the error), should be compared to the expected value[35] $M_0=n-m$, where n = number of angles θ_i at which measurements are made and m = number of parameters in the proposed fit (here 3). In general, the fits are poorer than expected. Either (1) or (2) could account for this. Four-constant analyses of the data do not significantly improve the fit in any case except the 150-Mev π^- elastic scattering, where the improvement is great, but probably accidental. With this one reservation, one can safely say that if there is a $\cos^3\theta$ contribution, it must be smaller than twice the error quoted for b in Table VI. The deviations are therefore random with respect to such a term, and should probably be ascribed to reason (2). There seems to be no point in investigating higher harmonics, whose presence in the absence of a $\cos^3\theta$ term would be hard to justify.

In conclusion it should be pointed out that we have not demonstrated that d wave scattering is very small. It could happen that d waves affect only the isotropic,

[34] Such a scatter would, for example, be produced if accidental coincidences contributed significantly and the duty cycle of the beam varied considerably.

[35] H. Cramér, *Mathematical Methods of Statistics* (Princeton University Press, Princeton, 1946).

$\cos\theta$, and $\cos^2\theta$ terms, their contribution to the $\cos^3\theta$ term being accidentally zero in our narrow energy range. This question could probably be decided by an accurate differential scattering experiment at somewhat higher energy.

IX. PHASE-SHIFT ANALYSIS

In the absence of any clear indication of a d wave in the angular distributions, we have made a preliminary phase shift analysis of the cross section data assuming that only s and p waves (of isotopic spin 1/2 and 3/2) are present in the scattered wave. As is well known,[3] this requires a representation of the data for the three scattering reactions in terms of six phase shifts, α_3, α_{33}, α_{31} for the states of isotopic spin 3/2 and angular momentum $s_{1/2}$, $p_{3/2}$, $p_{1/2}$, respectively, and α_1, α_{13}, α_{11} for states of corresponding angular momentum and of isotopic spin 1/2.

The phase shifts at each energy were found by a graphical method[24] using the nine coefficients a,b,c listed in Table VI for each of the three scattering processes. Table VII contains the results and shows the multiplicity of possible solutions. At 170 Mev, the π^+ coefficients just failed to produce the intersections required by the graphical method. After multiplying the coefficients by 0.97, corresponding to the indicated 3 percent uncertainty in the scale factor, and reducing the magnitude of the coefficient b_+ by its error, the two circles representing different loci of the point A $[=\exp(2i\alpha_3)-1]$ became tangent. The sensitivity of these loci to small changes in the π^+ coefficients, especially b_+, is readily understandable since the point $A+B$ on the graph is close to the real axis[36] and therefore dificult to locate accurately (since it depends on finding the intersection of a circle with a straight line to which it is almost tangent).

Table VII also contains phase shifts obtained by a variation of the ones resulting from the graphs. The graphical technique favors the π^+ data disproportionately so that it is possible to improve the fit of the

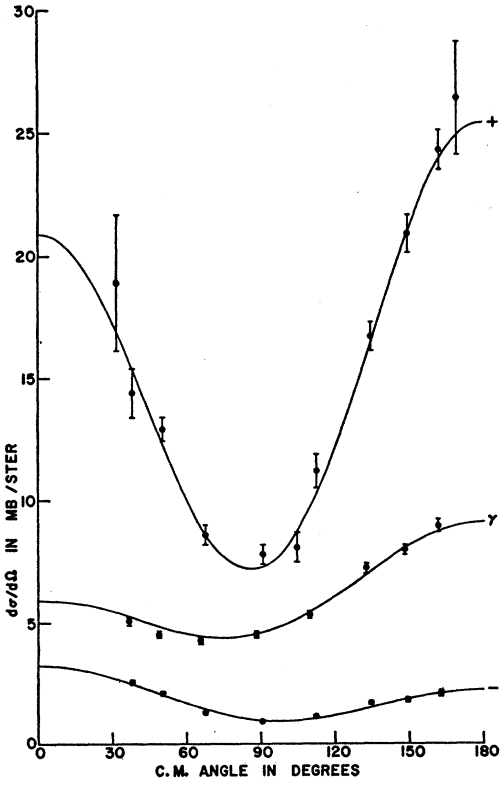

FIG. 4. 150-Mev pion-proton differential scattering cross sections. The curves represent the cross sections given by the phase shifts: $\alpha_3=-10°$, $\alpha_{33}=51.5°$, $\alpha_{31}=-5°$, $\alpha_1=9°$, $\alpha_{13}=2°$, $\alpha_{11}=2°$. The experimental points are plotted with the scale factors: $(+)\times0.97$, $(-)\times1.00$, $(\gamma)\times1.00$ (see Sec. VIII).

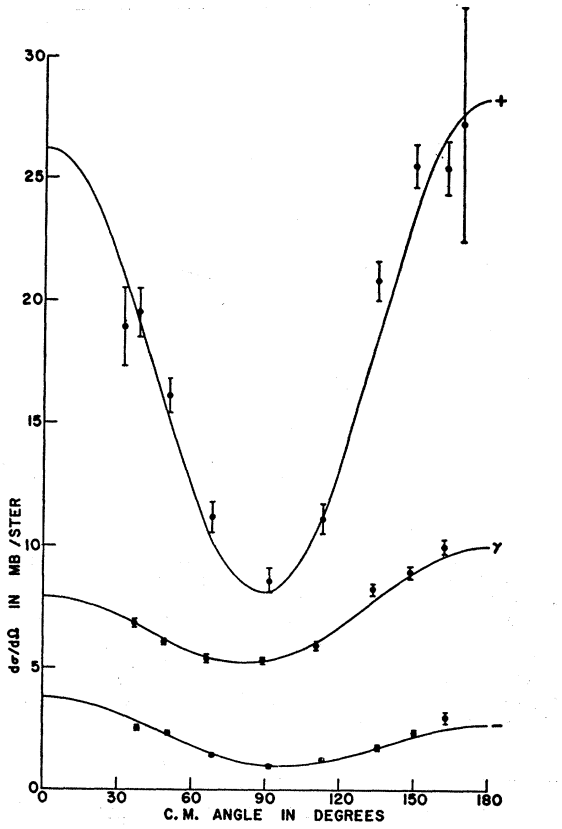

FIG. 5. 170-Mev pion-proton differential scattering cross sections. The curves represent the cross sections given by the phase shifts: $\alpha_3=-8°$, $\alpha_{33}=65°$, $\alpha_{31}=-8°$, $\alpha_1=10°$, $\alpha_{13}=2°$, $\alpha_{11}=0°$. The experimental points are plotted with the scale factors: $(+)\times0.97$, $(-)\times0.95$, $(\gamma)\times1.05$ (see Sec. VIII).

[36] This means that the real part of the forward scattering amplitude [proportional to $\mathrm{Im}(A+B)$] is small at this energy. Anderson, Davidon, and Kruse [Phys. Rev. **100**, 339 (1955)] have shown that this is to be expected on the basis of a general dispersion relation of M. L. Goldberger [Phys. Rev. **99**, 979 (1955)] giving the real part of the forward scattering amplitude in terms of an integral over all energy involving the total cross section. According to this relation the real part of the forward amplitude for π^+ scattering changes abruptly from positive to negative near 180 Mev.

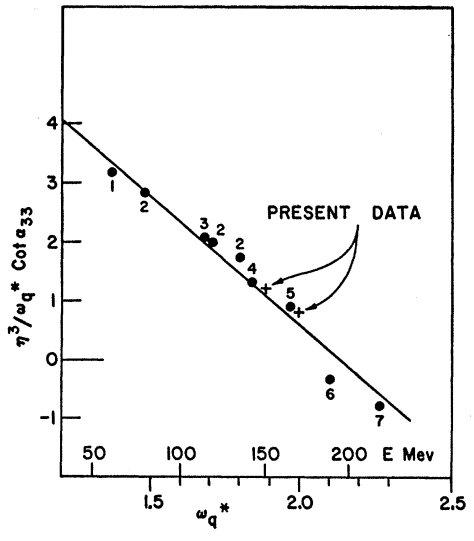

FIG. 6. Plot of $(\eta^3/\omega_q^*)\cot\alpha_{33}$ against ω_q^* (Chew and Low, reference 38). η is the center-of-mass momentum of the pion in units of μc and ω_q^* is the center-of-mass energy minus the proton rest energy in units of μc^2. 1: D. Bodansky *et al.*, reference 9; 2: H. L. Anderson *et al.*, reference 3; 3: J. Orear, Phys. Rev. **96**, 1417 (1954); 4: J. J. Lord and A. B. Weaver (quoted by Anderson, Davidon, and Kruse (reference 36); 5: H. L. Anderson and M. Glicksman, reference 5; 6: Anderson, Davidon, Glicksman, and Kruse, reference 6; 7: M. Glicksman, reference 4.

π^- coefficients at the expense of the π^+. This was done only for the set corresponding to that preferred by de Hoffmann *et al.*[37] in which α_{33} goes through a resonance. Figures 4 and 5 show the comparison of the differential cross sections given by these phase shifts and the experimental points (in some cases scaled up or down within the limits set for the scale factor in Table IV and Table V). To find the "best" set of phase shifts requires an electronic computer.

It is interesting to compare the phase shifts with those obtained in other experiments at neighboring energies.[5,6] In the case of α_{33}, the experimental values may be conveniently plotted on the graph proposed by Chew and Low[38] which predicts that approximately

$$(k^3/\omega_q^*)\cot\alpha_{33}=\text{const}(1-\omega_q^*/\omega_{\text{res}}),$$

where k is the momentum of the meson, ω_q^* is the total energy in the center-of-mass system minus the proton rest energy and ω_{res} is the value of ω_q^* for which α_{33} has the value 90°. Figure 6 shows the two points of this experiment together with the others. The linearity of the plot is quite striking.

The remaining p-wave phase shifts, α_{31}, α_{13}, and α_{11} show an erratic behavior in going from one experiment to another, and are generally small. The s-wave phase shifts α_1 and α_3 are less erratic but still allow many possible interpolations for their energy dependence. The values obtained in this experiment are in reasonable agreement with the linear extrapolations of Orear[39] $\alpha_1=0.16\eta$ and $\alpha_3=-0.11\eta$ (in radians), where η is the momentum of the meson in units of μc.

ACKNOWLEDGMENTS

We wish to thank J. Kunze and R. McIlwain for help in setting up the equipment and taking data.

[37] de Hoffmann, Metropolis, Alei, and Bethe, Phys. Rev. **95**, 1586 (1954).

[38] G. F. Chew and F. E. Low, Phys. Rev. (to be published), and *Proceedings of the Fifth Annual Rochester Conference on High Energy Physics* (University of Rochester Press, Rochester, 1955).

[39] J. Orear, Phys. Rev. **96**, 176 (1954) and **100**, 288 (1955).